ACS APPLIED MATERIALS & INTERFACES

Research Article

www.acsami.org

Large-Scale Fabrication of Commercially Available, Nonpolar Linear Polymer Film with a Highly Ordered Honeycomb Pattern

Van-Tien Bui,[†] Seung Hyeon Ko,[‡] and Ho-Suk Choi*[,†]

[†]Department of Chemical Engineering, Chungnam National University, 99 Daehak-ro, Yuseong-Gu, Daejeon 305-764, Republic of Korea

[‡]Institute for Basic Science, 70 Yuseong-daero 1689-gil, Yuseong-Gu, Daejeon 305-811, Republic of Korea

Supporting Information

ABSTRACT: Highly ordered, hexagonally patterned poly(methyl methacrylate) (PMMA) thin film is successfully fabricated using an improved phase separation method. A mixture of chloroform and methanol, which is used as a volatile solvent/nonsolvent pair, effectively controls the surface morphology and sensitively determines the ordered pattern. In particular, the methanol accumulation, which induces the formation of a gel-like protective layer and enhances the lateral capillary force, is crucial in the formation of the highly ordered hexagonal pattern even when using a nonpolar polymer such as PMMA. The convergence of cost-effective and large-scale production of highly ordered micropatterned film has wide potential for application, and it can enable new prospects for the commercialization of future high-tech devices that require specific multifunctionality.

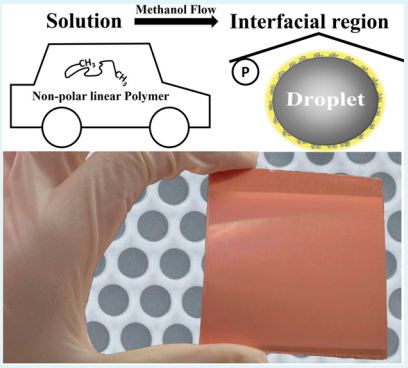

KEYWORDS: *methanol accumulation, phase separation, honeycomb film, ordered structure, poly(methyl methacrylate)*

INTRODUCTION

Highly ordered two-dimensional (2D) arrays of micropores with hexagonal honeycomb structures are of significant interest in many areas such as microtemplates,[1−3] membranes,[4,5] organic optoelectronics,[6−8] advanced electronics,[9,10] and tissue engineering.[11,12] Over the past few decades, a variety of top-down and bottom-up techniques, including lithography,[13−15] colloidal templates,[16] block copolymer phase separation,[17−19] emulsion,[20,21] and breath figure (BF),[22−26] have been developed to create ordered structures with uniform pore sizes in the nano- to micrometer range. Among these techniques, BF has become the most common technique for fabricating films with honeycomb micropore patterns due to its versatility and cost effectiveness.[22,23] In the BF approaches, the droplet stability and lateral capillary force are key factors that determine the ordered structure.[24] Thus, polymers with specifically designed structures such as block copolymers, comb-like copolymers, and amphiphilic polymers are good candidates because they can easily self-assemble at the interfacial region in order to prevent the coalescence of droplets.[24] The use of nanoparticles or surfactants as stabilizing agents is another strategy to promote droplet stability and yield high quality in patterned films.[27−32] However, nonpolar linear polymers cannot easily generate ordered structures without using nanoparticles or surfactants, because they are unable to form a polymer envelope to stabilize the droplets, which leads to coalescence and results in a structure with low regularity.[24] Indeed, only a few nonpolar linear polymers have been successful at fabricating films with honeycomb micropore patterns without using nanoparticles or surfactants as stabilizing agents. Furthermore, the creation of highly ordered micropore patterns is only possible under highly humid environments after drop-casting the polymer solution onto the substrate surface. These limitations have always become critical hurdles to commercially producing large-scale films with highly ordered honeycomb micropatterns.

Here, a simple and cost-effective two-step process is reported for fabricating films with highly ordered micropore patterns under ambient air conditions while using commercially available polymers including nonpolar polymers such as poly(methyl methacrylate) and polystyrene. The first step in the process is the conventional coating of the polymer solution on a solid substrate in order to fabricate a large-scale thin polymer film with a uniform thickness. The second step is a quick dip-coating of a mixture of highly volatile solvent (chloroform, ChL) and nonsolvent (methanol, MeOH) on the surface of the thin polymer film. The evaporation of the mixture under ambient air eventually induces phase separation and spontaneously creates a thin polymer film with a highly ordered honeycomb micropattern.

EXPERIMENTAL SECTION

Materials. Commercially available polymer pellets including PMMA (PMMA EG920) and PS (GPPS 15NFI) were purchased

Received: March 10, 2015
Accepted: April 29, 2015
Published: April 29, 2015

DOI: 10.1021/acsami.5b02097
ACS Appl. Mater. Interfaces 2015, 7, 10541−10547

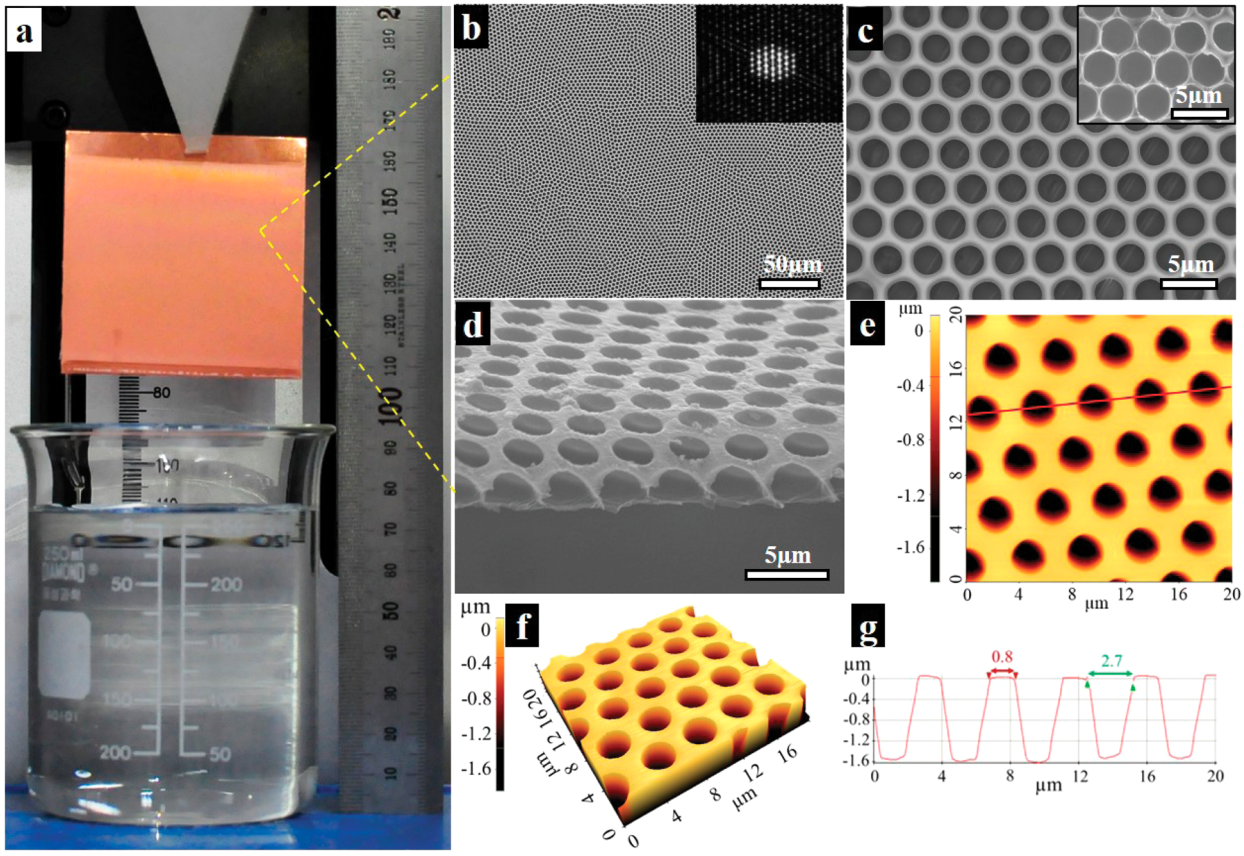

Figure 1. (a) Large-scale fabrication of the honeycomb film. Here, b–g present the surface morphologies of the typically patterned films prepared with a solvent/nonsolvent volume ratio of 85/15 under an ambient air environment (i.e., relative humidity of 55% and temperature of 23 °C): (b) low-magnification FESEM image with the FFT pattern in the inset, (c) high-magnification FESEM image, (d) cross-sectional FESEM image, (e, f) 2D and 3D AFM images, respectively, and (g) cross-sectional profile of e. The inset of c is a FESEM image of the patterned pincushion film. The red line in e indicates the location of the cross-sectional profile.

from LG Chem Co. (Seoul, Korea). Poly(lactic acid) (PLA) was purchased from NatureWorks (Minnetonka, MN, USA). They were first dried in a vacuum oven at 60 °C. Poly(4-styrene sulfonic acid) (PSS, $M_w \sim 75{,}000$, 18 wt % in H_2O) was purchased from Sigma-Aldrich (St. Louis, MO, USA). Copper substrates (thickness, 0.5 mm) were obtained from 4Science (Seoul, Korea). These substrates were successively washed with a 0.1 M sulfuric acid solution and distilled water followed by blow-drying in nitrogen gas prior to use. Chloroform (anhydrous, with amylenes as stabilizers; 99.8%) and methanol (anhydrous; 99.8%) were purchased from Sigma-Aldrich and used as received.

Preparation of Porous Structures. In the first step, a homogeneous solution containing 10 wt % PMMA in ChL was prepared. Then, the polymer solution was coated onto the copper substrate via spin-coating (1000 rpm for the first 10 s and 3000 rpm for the following 30 s), and it was left in ambient air to completely evaporate the solvent, which resulted in the formation of a thin polymer film with a uniform thickness. For large-area fabrication, other coating techniques can be employed, including bar or roll coatings, as long as the air humidity and solution viscosity are controlled. The binary mixtures of the solvent/nonsolvent were prepared with different volume ratios of ChL and MeOH and were stirred continuously for 24 h before use. The patterned porous structure was fabricated using the method available in the literature.[33] Briefly, the polymer film coated on the copper substrate was dipped into a mixture of solvent and nonsolvent for 5 s using a dip-coater (E-flex, Seoul, Korea). Then, the specimen was withdrawn from the solvent mixture, and the residual solvent on the surface of the specimen was allowed to evaporate completely under ambient air conditions. The optimum dipping conditions were a dipping speed of 50 mm/min and a withdrawal speed of 60 mm/min. The humidity and temperature controller (TH-TG-1000, Jeio Tech, Seoul, Korea) was used to precisely control the ambient humidity and temperature.

Preparation of Membranes. The procedure was the same as that for the preparation of the porous structure, except that an additional sacrificial layer between the copper substrate and PMMA thin film was used. The sacrificial layer is necessary not only in order to easily detach the thin PMMA film from the copper substrate but also for efficiently generating a through-pore structure. In order to fabricate the additional sacrificial layer, a solution containing 10 wt % PSS in methanol was prepared first. The PMMA/PSS bilayer was prepared through sequentially coating PSS and PMMA onto the copper substrate using the spin-coating method. First, the PSS solution in methanol was coated onto the copper substrate via spin-coating, and then the coating was dried completely in a vacuum oven at 70 °C. Second, the polymer solution in chloroform was continuously coated onto the PSS/copper surface and left in air for complete drying. Because PSS is not dissolved in chloroform, the PSS precoating is stable in polymer solutions. Thus, a bilayer of polymer and polyelectrolyte (PSS) can be prepared. Next, the bilayer of PMMA/PSS coated onto the copper surface was exposed to the solvent mixture (ChL/MeOH) to induce a phase separation using the same procedure as discussed in the previous section. After drying completely, the honeycomb structure was formed. Finally, the freestanding polymer film with through-pores can be obtained after removing the PSS layer through immersing the sample in water for several minutes.

Characterization. The morphology of the obtained specimen was characterized using a field emission scanning electron microscope (FESEM; JEOL, JSM-7000F, Tokyo, Japan) and atomic force

DOI: 10.1021/acsami.5b02097
ACS Appl. Mater. Interfaces 2015, 7, 10541–10547

microscope (AFM; Pork Science Instruments Autroprobe CP). The static contact angle measurement was performed using a drop shape analyzer (Krüss DSA 100, Hamburg, Germany). Distilled water (DW) was used as the probe liquid for this measurement, and a minimum of five readings were averaged.

RESULTS AND DISCUSSION

The optical image in Figure 1a demonstrates the potential for the proposed strategy to be expanded to large-scale production of honeycomb micropatterned films. The film was prepared with a ChL/MeOH volume ratio of 85/15 in an ambient air environment. The homogeneous sample color reflects the high uniformity of the patterned film, which was observed throughout the coated surface (~30 cm^2). Parts b and c of Figure 1 demonstrate a relatively large area and a perfectly ordered array of the hexagonal micropore domains, respectively. The fast Fourier transform (FFT) analysis, as depicted in the inset of Figure 1b, further confirmed the long-range hexagonally ordered array. The monodispersed pore array was uniformly formed with a diameter of 2.7 μm and an interval of 0.8 μm. The inset of Figure 1c illustrates the surface morphology after peeling off the top layer of the honeycomb film, which demonstrates that each pore has a spherical jar shape with an internal diameter of 3.5 μm. Figure 1d presents a cross-sectional image of the honeycomb film, which exhibits a monolayer of pore arrays on the substrate surface. Each pore is closed at one end, and they are isolated from each other. The thickness of the film was approximately 1.7 μm, which is slightly larger than the pore depth (1.6 μm) due to the bottom thin layer inside the pore. For more insight into the geometry, the 2D and 3D AFM images are also presented in Figures 1e,f, respectively. As seen in Figure 1g, the scan profile at a cross-section of Figure 1e further confirms the diameter, interval, and depth of the pores.

It is known that phase separation can be realized with the introduction of a nonsolvent to the polymer solution.[34,35] The locally concentrated methanol-rich phase, which is induced by the solvent evaporation, is responsible for the phase separation; in this case, the water that condensed from air to a nonsolvent assists in growing the nonsolvent droplets, which in turn enable the formation of the honeycomb pattern on the polymer film.[33] When a nonsolvent is used in conjunction with a solvent, it has dual roles of increasing the number of nucleation sites and reducing the crystallization time of the polymer through increasing the extent of the phase separation. Accordingly, the nonsolvent content can be expected to determine the aggregate size or pore volume of the resulting porous structure. Thus, the pore size, pore density (number of pores per area), and conformational entropy of the patterned film were thoroughly characterized at various compositions in order to investigate the influence of the ChL/MeOH compositions on the surface morphology.

Figure 2 presents the FESEM images of the PMMA film surfaces prepared with different compositions of ChL/MeOH under an evaporation temperature of 20 °C and a relative humidity (RH) level of 60%. An experiment using only ChL without adding a nonsolvent resulted in a random distribution of many irregular pores with a mean pore diameter of 1.03 ± 0.23 μm, as seen in Figure 2a. This result indicates that only water droplets, randomly condensed from ambient air during the ChL evaporation as in the BF technique, are not sufficient to generate many uniform micropores. At a MeOH content of 10%, there were many micropores with a poor distribution

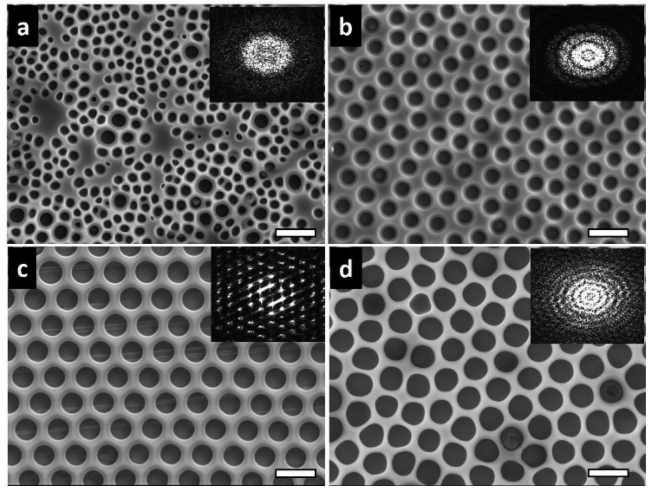

Figure 2. FESEM images of the film surfaces prepared with various solvent/nonsolvent volume ratios of (a) 100/0, (b) 90/10, (c) 85/15, and (d) 80/20. The inset in each image is the corresponding FFT pattern. Scale bar: 5 μm.

(also supported by the FFT image in the inset of Figure 2b) but a nearly uniform size of 1.89 ± 0.1 μm was formed over the film area, as depicted in Figure 2b. This indicates that a small amount of MeOH in the ChL/MeOH solution has a crucial function in the formation of uniform micropores. At a MeOH content of 15%, a highly ordered 2D array of micropores with a hexagonal honeycomb structure was obtained, as seen in Figure 2c and the FFT image in the inset. The average pore diameter was 2.72 ± 0.06 μm; this results in a small relative standard deviation of 2.2%, which demonstrates the high uniformity of their size. Because all micropores were not only uniform in size but also regularly distributed over the surface, a ChL/MeOH volume ratio of 85/15 appears to be the most appropriate ratio for fabricating a thin PMMA film with a highly ordered honeycomb micropattern. However, further increases in the MeOH content to 20% generated fewer ordered structures with a low uniformity in pore size, as seen in Figure 2d. The average pore diameter increased to 3.01 ± 0.21 μm due to the increase in the MeOH content, while the thickness of the pore wall decreased. Briefly, the methanol content of 15% is the optimum concentration for generating the best quality of patterned PMMA films, which is supported by the smallest values of the standard deviation and conformational entropy, as listed in Table 1.

The change in the surface morphology with varying solvent compositions was also confirmed through analyzing the wetting properties of the resulting films, as seen in Figure 3. From a macroscopic perspective, the apparent contact angle was typically used to qualify the surface wettability, which is

Table 1. Effect of Methanol Content on the Mean Pore Diameter, Standard Deviation of Pore Diameters, Number Density, and Entropy

solvent composition	pore size (μm)	std dev (μm)	pore density (pores × $10^{-3}/\mu m^2$)	entropy
ChL/MeOH = 100/0	1.03	0.23	344.0	1.265
ChL/MeOH = 90/10	1.89	0.10	107.5	0.933
ChL/MeOH = 85/15	2.72	0.06	80.2	0.079
ChL/MeOH = 80/20	3.01	0.21	72.0	0.583

DOI: 10.1021/acsami.5b02097
ACS Appl. Mater. Interfaces 2015, 7, 10541−10547

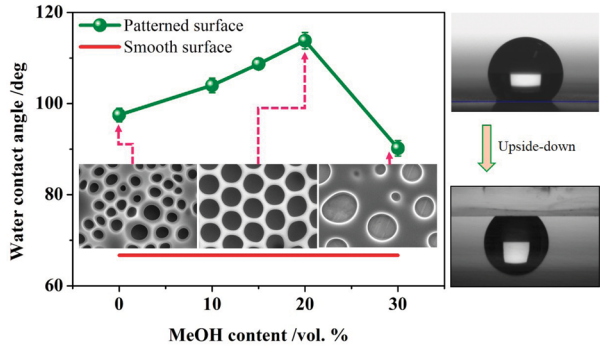

Figure 3. Wetting properties of the patterned films prepared with various compositions of solvent/nonsolvent pairs. The photograph on the right represents the high adhesion force between the droplet and patterned surface.

governed by the surface roughness and surface chemistry. The water contact angle of the smooth PMMA film was ~68.5°, which indicated that PMMA was inherently hydrophilic. Figure 3 depicts the variation of the water contact angle as a function of the MeOH content. The contact angle increased with increasing MeOH content and reached a maximum value (~118°) at 20 vol. %. Subsequently, the contact angle began decreasing when the MeOH content was more than 20 vol. %. This can be explained by the effect of air trapped within the cavities of the porous surface on the increase of the apparent contact angle. In the Cassie–Baxter theory, which is applied in porous structures,[36] air pockets are assumed to be trapped underneath liquid droplets, which represent a composite surface. Defining the apparent contact angle in the Cassie mode as θ_c, θ_c can be correlated to the surface solid fraction using the following equation:

$$\cos\theta_c = f_s(\cos\theta_s + 1) - 1$$

where f_s and θ_s are the surface solid fraction and the contact angle of the smooth surface. The apparent contact angle increases with increases in the surface roughness. Thus, the increase of the water contact angle can be ascribed to the enhancement of the pore volume of the microporous surface. Interestingly, the porous patterned surface exhibited high adhesion with liquid droplets as seen in the photos on the right of Figure 3. The highly adhesive force of the microporous surface with the water droplet can be explained using the Cassie impregnating wetting state and the negative pressure caused by the volume change of air sealed in the micropores.[37,38]

The pore size of the patterned film can be further fine-tuned through modulating of the experimental processing conditions such as the ambient humidity level, evaporation temperature, concentration of the coating solution, and withdrawal speed of the film from the solvents (Supporting Information Figures S1–S4). Briefly, the ordered patterns could be formed within an RH range of 40–80% and a temperature range of 10–30 °C. The concentration of the polymer coating solution should be in the range of 5–15 wt %, in which the polymer solution revealed suitable viscosity during the coating process. The pore size can be increased through increasing the RH levels or reducing the evaporation temperature. The withdrawal speed (i.e., pulling the specimen out from the solvent/nonsolvent solution) should be 60 mm/s in order to acquire a sufficient thickness for the coating film.

In order to understand the advantages of the newly developed strategy over the conventional BF approaches, the role of methanol was further investigated in the stabilization of the nonsolvent droplets and in the enhancement of the lateral capillary force between the adjacent droplets, which was beneficial to the formation of the ordered structures. Figure 4a

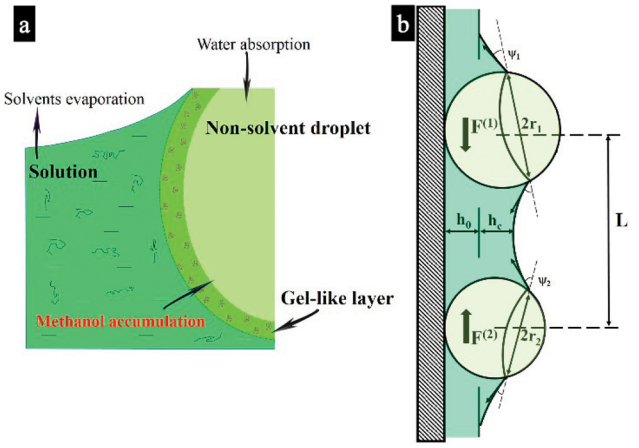

Figure 4. Schemes illustrating (a) the methanol accumulation that induced the formation of the gel-like layer and (b) the origin of the lateral capillary forces induced via deformation of the solution surface when the film is thin.

presents the formation of the nonsolvent droplets. The solvent evaporation induced not only water absorption from air but also methanol accumulation from the solution. The mass transfer of methanol induced the transport of some polymer molecules to the interfacial region between a continuous solution phase and a dispersed droplet phase. The polymer molecules in the interfacial region must change their conformation from swollen coils to collapsed globules as a result of the influence of the nonsolvent.[34,35] The collapsed polymer molecules function as nanoparticles. Thus, the interfacial region eventually has a gel-like state and finally functions as a protective layer, which stabilizes the droplets from the coalescence and results in high regularity of the pores. Because the solvents used in the conventional BFs are commonly immiscible with water,[22−26] there is no mass transfer from the solution to the droplets. Consequently, nonpolar linear polymers do not have the potential to form a gel-like protective layer. This is the primary reason for the lower regularity of the structures prepared using nonpolar linear polymers through the conventional BF technique. Moreover, the methanol accumulation can also enhance the lateral capillary force between adjacent droplets. Theoretically, the deformation of the solution surface by nonsolvent-rich droplets results in capillary forces, as represented in Figure 4b. The lateral capillary force between two droplets with radii of R_1 and R_2 separated by a center-to-center distance (L) is expressed as follows:[39,40]

$$F = \frac{-2\pi\sigma Q_1 Q_2}{L} \qquad (1)$$

where σ is the interfacial tension of the solution and droplets, r_1 and r_2 are the radii of the two contact lines, and Q_1 and Q_2 are the "capillary charges", which are defined as follows:

$$Q_i = r_i \sin\psi_i \qquad (i = 1, 2) \qquad (2)$$

DOI: 10.1021/acsami.5b02097
ACS Appl. Mater. Interfaces 2015, 7, 10541–10547

where ψ_1 and ψ_2 are the meniscus slope angles at the two contact lines. After substituting eq 2 into eq 1, it can be easily concluded that the lateral capillary force is directly proportional to the radii of the two droplets ($F \sim R_1R_2$). More methanol accumulation induces larger droplets, which results in a stronger capillary force. Thus, the capillary force is sufficiently strong to induce aggregation and ordering of droplets. This is consistent with the experimental observations in the 2D micropore array, which revealed better ordering of the honeycomb pattern with larger pore sizes as the MeOH content increased from 10% to 15% in the solution, as described in Figure 2 and Table 1.

In order to demonstrate the advantages of the proposed strategy over the conventional BF technique, a honeycomb film was fabricated under harsh conditions, including low humidity. The highly ordered honeycomb film was obtained even when it was prepared in a confined region inside a small open-ended tube, as depicted in Figure 5a,b. This can be a significant challenge for BF techniques because it is difficult to provide humid air in confined regions with curvature. The proposed strategy was also successful in fabricating ordered patterns from other common polymers such as PS and PLA, as presented in Figure 5c,d. Considering the cross-linkability of PS and the excellent biocompatibility of PLA, the proposed strategy could have significant potential to extend the application of honeycomb films to areas that require more specific multifunctionality. Moreover, a variety of common substrates such as glass, copper, wrapped foil, and plastic could be used to prepare ordered patterns in polymer films (Supporting Information Figure S5).

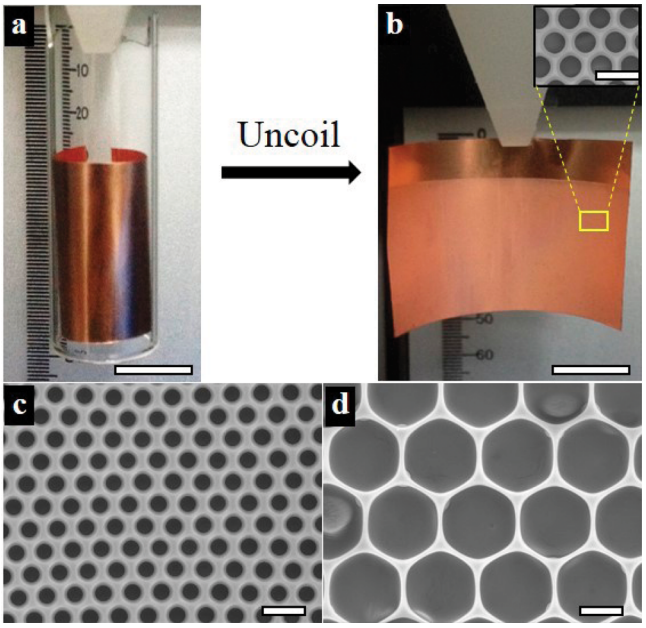

Figure 5. (a) Coiled PMMA film coated on a copper substrate inserted inside an open-ended glass tube (the coating surface was exposed to air) and (b) the uncoiled film after the solvent treatment. The inset of b is the corresponding FESEM image of the patterned film. FESEM images of the honeycomb patterned film prepared from (c) PS and (d) PLA in an ambient air environment (i.e., relative humidity of 55% and temperature of 23 °C). The solvent/nonsolvent volume ratio was 85/15 for PMMA and PLA patterned films and 90/10 for the PS film. The scale bars in a and b are 2 cm; those in the inset of b, in c, and in d are 5 μm.

It is worthy to note that the highly ordered honeycomb film with through-pores can be realized from the phase separation of polymer solution at the interface of water-soluble polyelectrolyte-coated copper substrates, as shown in Figure 6. Films with through-pores have exhibited significant potential as size-selective membranes and masks.[4,41,42] To date, size-selective microporous membranes are usually fabricated using the BF method through casting a dilute solution of an expensive copolymer at a water/air or ice/air interface.[4,5] However, the casting technique possesses a limit of creating a large-scale film with a uniform thickness resulting from the surface tension of the polymer solution. Through exploiting the solution precoating, a large-scale, uniform polymer film can be prepared on the polyelectrolyte surface, which enables massive production of membranes. The calculations by Wan et al. indicate that the interfacial tension of soft substrates is essential for the formation of honeycomb films with through-pores.[4] The polyelectrolyte sacrificial layer used in the proposed strategy can be dissolved in water or methanol, which are the main components of the nonsolvent droplet. Thus, further penetration of the nonsolvent droplets into the sacrificial layer leads to stable formation of the honeycomb topcoat layer with through-pores. Because the proposed strategy can also be applied to other commercially available polymers with different mechanical properties, it can be a useful technique for producing size-selective microporous membranes with large areas.

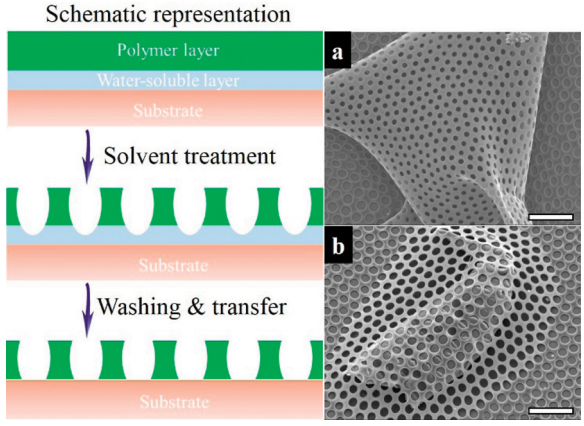

Figure 6. Schemes illustrating the fabrication of a microporous membrane via an improved phase separation method. FESEM images present (a) a wrinkled membrane and (b) a membrane covering over dust. Scale bars are 20 μm.

CONCLUSION

A simple and cost-effective strategy for producing microporous honeycomb films with highly ordered hexagonal structures using various commercially available polymers, including nonpolar linear polymers such as PMMA, has been reported. All fabrication steps were conducted under an ambient air environment without providing additional humid air or using stabilizing agents. The mixture of ChL/MeOH, which was used as a volatile solvent/nonsolvent pair, effectively controlled the surface morphology as well as sensitively determined the quality of the patterned film. The ChL/MeOH volume ratio of 85/15 was demonstrated to be the most appropriate ratio for fabricating thin PMMA films with highly ordered honeycomb micropatterns. The pore size could also be controlled through

DOI: 10.1021/acsami.5b02097
ACS Appl. Mater. Interfaces 2015, 7, 10541−10547

adjusting the compositions of the solvent pairs and modulating the experimental processing conditions. Moreover, it was demonstrated that the methanol accumulation, which induces the formation of gel-like protective layers and enhances the lateral capillary force, is responsible for the regularly ordered structures of the nonpolar polymers. The convergence of cost-effective and large-scale production of highly ordered micropatterned film has wide potential for application, and it can enable new prospects for the commercialization of future high-tech devices that require specific multifunctionality.

■ ASSOCIATED CONTENT

Supporting Information

Effect of experimental conditions on surface morphology including humidity, temperature, solution concentration, substrate, and withdrawing speed. The Supporting Information is available free of charge on the ACS Publications website at DOI: 10.1021/acsami.5b02097.

■ AUTHOR INFORMATION

Corresponding Author

*E-mail: hchoi@cnu.ac.kr.

Notes

The authors declare no competing financial interest.

■ ACKNOWLEDGMENTS

This research was supported by a grant from the National Research Foundation (NRF) grant funded by the Korean government (MSIP; NRF-2014R1A2A2A01006994) and by the Technology Innovation Program (Grant G01201406010606) funded by the Ministry of Trade, Industry & Energy (MOTIE, Korea).

■ REFERENCES

(1) de Boer, B.; Stalmach, U.; Nijland, H.; Hadziioannou, G. Microporous Honeycomb-Structured Films of Semiconducting Block Copolymers and Their Use as Patterned Templates. *Adv. Mater.* **2000**, *12*, 1581−1583.

(2) Li, L.; Zhong, Y.; Ma, C.; Li, J.; Chen, C.; Zhang, A.; Tang, D.; Xie, S.; Ma, Z. Honeycomb-Patterned Hybrid Films and Their Template Applications via a Tunable Amphiphilic Block Polymer/Inorganic Precursor System. *Chem. Mater.* **2009**, *21*, 4977−4983.

(3) Connal, L. A.; Qiao, G. G. Preparation of Porous Poly(dimethylsiloxane)-Based Honeycomb Materials with Hierarchal Surface Features and Their Use as Soft-Lithography Templates. *Adv. Mater.* **2006**, *18*, 3024−3028.

(4) Wan, L.-S.; Li, J.-W.; Ke, B.-B.; Xu, Z.-K. Ordered Microporous Membranes Templated by Breath Figures for Size-Selective Separation. *J. Am. Chem. Soc.* **2011**, *134*, 95−98.

(5) Cong, H.; Wang, J.; Yu, B.; Tang, J. Preparation of a Highly Permeable Ordered Porous Microfiltration Membrane of Brominated Poly(phenylene oxide) on an Ice Substrate by the Breath Figure Method. *Soft Matter* **2012**, *8*, 8835−8839.

(6) Shimomura, M.; Koito, T.; Maruyama, N.; Arai, K.; Nishida, J.; Gråsjö, L.; Karthaus, O.; Ijiro, K. Photonic and Electronic Applications of Mesoscopic Polymer Assemblies. *Mol. Cryst. Liq. Cryst.* **1998**, *322*, 305−312.

(7) Freymann, G. von; Kitaev, V.; Lotsch, B. V.; Ozin, G. A. Bottom-up Assembly of Photonic Crystals. *Chem. Soc. Rev.* **2013**, *42*, 2528−2554.

(8) Noda, S.; Chutinan, A.; Imada, M. Trapping and Emission of Photons by a Single Defect in a Photonic Bandgap Structure. *Nature* **2000**, *407*, 608−610.

(9) Saunders, A. E.; Shah, P. S.; Sigman, M. B.; Hanrath, T.; Hwang, H. S.; Lim, K. T.; Johnston, K. P.; Korgel, B. A. Inverse Opal Nanocrystal Superlattice Films. *Nano Lett.* **2004**, *4*, 1943−1948.

(10) Liu, X.; Jung, H.-G.; Kim, S.-O.; Choi, H.-S.; Lee, S.; Moon, J. H.; Lee, J. K. Silicon/Copper Dome-Patterned Electrodes for High-Performance Hybrid Supercapacitors. *Sci. Rep.* **2013**, DOI: 10.1038/srep03183.

(11) Yamamoto, S.; Tanaka, M.; Sunami, H.; Ito, E.; Yamashita, S.; Morita, Y.; Shimomura, M. Effect of Honeycomb-Patterned Surface Topography on the Adhesion and Signal Transduction of Porcine Aortic Endothelial Cells. *Langmuir* **2007**, *23*, 8114−8120.

(12) Zhu, Y.; Sheng, R.; Luo, T.; Li, H.; Sun, J.; Chen, S.; Sun, W.; Cao, A. Honeycomb-Structured Films by Multifunctional Amphiphilic Biodegradable Copolymers: Surface Morphology Control and Biomedical Application as Scaffolds for Cell Growth. *ACS Appl. Mater. Interfaces* **2011**, *3*, 2487−2495.

(13) Moreau, W. M. *Semiconductor Lithography: Principles, Practices, and Materials (Microdevices)*; Plenum: New York, 1988.

(14) Qin, D.; Xia, Y.; Whitesides, G. M. Soft Lithography for Micro- and Nanoscale Patterning. *Nat. Protoc.* **2010**, *5*, 491−502.

(15) Kim, E.; Xia, Y.; Whitesides, G. M. Polymer Microstructures Formed by Molding in Capillaries. *Nature* **1995**, *376*, 581−584.

(16) Pernites, R. B.; Foster, E. L.; Felipe, M. J. L.; Robinson, M.; Advincula, R. C. Patterned Surfaces Combining Polymer Brushes and Conducting Polymer via Colloidal Template Electropolymerization. *Adv. Mater.* **2011**, *23*, 1287−1292.

(17) Wu, S.; Bubeck, C. Macro- and Microphase Separation in Block Copolymer Supramolecular Assemblies Induced by Solvent Annealing. *Macromolecules* **2013**, *46*, 3512−3518.

(18) Bang, J.; Jeong, U.; Ryu, D. Y.; Russell, T. P.; Hawker, C. J. Block Copolymer Nanolithography: Translation of Molecular Level Control to Nanoscale Patterns. *Adv. Mater.* **2009**, *21*, 4769−4792.

(19) Tung, S.-H.; Kalarickal, N. C.; Mays, J. W.; Xu, T. Hierarchical Assemblies of Block-Copolymer-Based Supramolecules in Thin Films. *Macromolecules* **2008**, *41*, 6453−6462.

(20) Imhof, A.; Pine, D. J. Ordered Macroporous Materials by Emulsion Templating. *Nature* **1997**, *389*, 948−951.

(21) Imhof, A.; Pine, D. J. Uniform Macroporous Ceramics and Plastics by Emulsion Templating. *Chem. Eng. Technol.* **1998**, *21*, 682−685.

(22) Bai, H.; Du, C.; Zhang, A.; Li, L. Breath Figure Arrays: Unconventional Fabrications, Functionalizations, and Applications. *Angew. Chem., Int. Ed.* **2013**, *52*, 12240−12255.

(23) Hernández-Guerrero, M.; Stenzel, M. H. Honeycomb Structured Polymer Films via Breath Figures. *Polym. Chem.* **2012**, *3*, 563−577.

(24) Wan, L.-S.; Zhu, L.-W.; Ou, Y.; Xu, Z.-K. Multiple Interfaces in Self-Assembled Breath Figures. *Chem. Commun. (Cambridge, U. K.)* **2014**, *50*, 4024−4039.

(25) Heng, L.; Wang, B.; Li, M.; Zhang, Y.; Jiang, L. Advances in Fabrication Materials of Honeycomb Structure Films by the Breath-Figure Method. *Materials* **2013**, *6*, 460−482.

(26) Bunz, U. H. F. Breath Figures as a Dynamic Templating Method for Polymers and Nanomaterials. *Adv. Mater.* **2006**, *18*, 973−989.

(27) Böker, A.; Lin, Y.; Chiapperini, K.; Horowitz, R.; Thompson, M.; Carreon, V.; Xu, T.; Abetz, C.; Skaff, H.; Dinsmore, A. D.; Emrick, T.; Russell, T. P. Hierarchical Nanoparticle Assemblies Formed by Decorating Breath Figures. *Nat. Mater.* **2004**, *3*, 302−306.

(28) Yin, S.; Goldovsky, Y.; Herzberg, M.; Liu, L.; Sun, H.; Zhang, Y.; Meng, F.; Cao, X.; Sun, D. D.; Chen, H.; Kushmaro, A.; Chen, X. Functional Free-Standing Graphene Honeycomb Films. *Adv. Funct. Mater.* **2013**, *23*, 2972−2978.

(29) Sun, W.; Ji, J.; Shen, J. Rings of Nanoparticle-Decorated Honeycomb-Structured Polymeric Film: The Combination of Pickering Emulsions and Capillary Flow in the Breath Figures Method. *Langmuir* **2008**, *24*, 11338−11341.

(30) Fan, D.; Jia, X.; Tang, P.; Hao, J.; Liu, T. Self-Patterning of Hydrophobic Materials into Highly Ordered Honeycomb Nanostructures at the Air/Water Interface. *Angew. Chem.* **2007**, *119*, 3406−3409.

(31) Ma, H.; Cui, J.; Song, A.; Hao, J. Fabrication of Freestanding Honeycomb Films with Through-Pore Structures via Air/Water Interfacial Self-Assembly. *Chem. Commun. (Cambridge, U. K.)* **2011**, *47*, 1154−1156.
(32) Saito, Y.; Shimomura, M.; Yabu, H. Dispersion of Al_2O_3 Nanoparticles Stabilized with Mussel-Inspired Amphiphilic Copolymers in Organic Solvents and Formation of Hierarchical Porous Films by the Breath Figure Technique. *Chem. Commun. (Cambridge, U. K.)* **2013**, *49*, 6081−6083.
(33) Bui, V.-T.; Ko, S. H.; Choi, H.-S. A Surfactant-Free Bio-Compatible Film with a Highly Ordered Honeycomb Pattern Fabricated via an Improved Phase Separation Method. *Chem. Commun. (Cambridge, U. K.)* **2014**, *50*, 3817−3819.
(34) Wang, D.-M.; Lai, J.-Y. Recent Advances in Preparation and Morphology Control of Polymeric Membranes Formed by Nonsolvent Induced Phase Separation. *Curr. Opin. Chem. Eng.* **2013**, *2*, 229−237.
(35) Guillen, G. R.; Pan, Y.; Li, M.; Hoek, E. M. V. Preparation and Characterization of Membranes Formed by Nonsolvent Induced Phase Separation: A Review. *Ind. Eng. Chem. Res.* **2011**, *50*, 3798−3817.
(36) Cassie, A. B. D.; Baxter, S. Wettability of Porous Surfaces. *Trans. Faraday Soc.* **1944**, *40*, 546−551.
(37) Feng, L.; Zhang, Y.; Xi, J.; Zhu, Y.; Wang, N.; Xia, F.; Jiang, L. Petal Effect: A Superhydrophobic State with High Adhesive Force. *Langmuir* **2008**, *24*, 4114−4119.
(38) Lai, Y.; Gao, X.; Zhuang, H.; Huang, J.; Lin, C.; Jiang, L. Designing Superhydrophobic Porous Nanostructures with Tunable Water Adhesion. *Adv. Mater.* **2009**, *21*, 3799−3803.
(39) Kralchevsky, P. A.; Nagayama, K. Capillary Interactions between Particles Bound to Interfaces, Liquid Films and Biomembranes. *Adv. Colloid Interface Sci.* **2000**, *85*, 145−192.
(40) Kralchevsky, P. A.; Nagayama, K. Capillary Forces between Colloidal Particles. *Langmuir* **1994**, *10*, 23−36.
(41) Ou, Y.; Zhu, L.-W.; Xiao, W.-D.; Yang, H.-C.; Jiang, Q.-J.; Li, X.; Lu, J.-G.; Wan, L.-S.; Xu, Z.-K. Nonlithographic Fabrication of Nanostructured Micropatterns via Breath Figures and Solution Growth. *J. Phys. Chem. C* **2014**, *118*, 4403−4409.
(42) Ma, C.-Y.; Zhong, Y.-W.; Li, J.; Chen, C.-K.; Gong, J.-L.; Xie, S.-Y.; Li, L.; Ma, Z. Patterned Carbon Nanotubes with Adjustable Array: A Functional Breath Figure Approach. *Chem. Mater.* **2010**, *22*, 2367−2374.

DOI: 10.1021/acsami.5b02097
ACS Appl. Mater. Interfaces 2015, 7, 10541−10547